DOI: 10.1021/ic9005289

Inorganic Chemistry
Article

Synthesis of Tetranuclear Rhodium and Iridium Complexes Directed by 6-Mercaptopyridin-2-ol: Electrochemical Behavior, Chemical Oxidation, and Coordination Chemistry

Pablo J. Alonso,[‡] Oscar Benedí,[†] María J. Fabra,[†] Fernando J. Lahoz,[†] Luis A. Oro,*[,†] and Jesús J. Pérez-Torrente*[,†]

[†]*Departamento de Química Inorgánica, Instituto Universitario de Catálisis Homogénea, Instituto de Ciencia de Materiales de Aragón, Universidad de Zaragoza-C.S.I.C., E-50009 Zaragoza, Spain, and* [‡]*Departamento de Física de la Materia Condensada, Instituto de Ciencia de Materiales de Aragón, Universidad de Zaragoza-C.S.I.C., E-50009 Zaragoza, Spain*

Received March 18, 2009

The new ligand 6-mercapto-2(1*H*)-pyridone (H_2PySO) has been prepared in good yield by reaction of 6-chloro-pyridin-2-ol with NaSH. Reaction of the salt K_2PySO, generated in situ, with the appropriate complex $[M(\mu\text{-Cl})(\text{diolefin})]_2$ affords the tetranuclear complexes $[M_4(\mu\text{-PySO})_2(\text{diolefin})_4]$ [M = Rh, diolefin = 1,5-cyclooctadiene (cod) (**1**), tetrafluorobenzobarralene (tfbb) (**2**); M = Ir, diolefin = cod (**3**)]. The molecular structure of complex **1** has been determined by X-ray diffraction methods. The tetranuclear structure is supported by two *S,N,O*-tridentate ligands exhibiting a $1\kappa O$, $2\kappa N$, $3{:}4\kappa^2 S$ coordination mode. Carbonylation of the rhodium diolefin complexes at atmospheric pressure gives $[Rh_4(\mu\text{-PySO})_2(CO)_8]$ (**4**). The carbonylation of **1** is partially reversible, and the mixed-ligand complex $[Rh_4(\mu\text{-PySO})_2(cod)_2(CO)_4]$ (**5**) has been obtained as a single isomer. The reaction of **4** with triphenylphosphine gives the compound $[Rh_4(\mu\text{-PySO})_2(CO)_4(PPh_3)_4]$ (**6**) which also exists as a single isomer of C_2 symmetry. The diolefin complexes are redox active and exhibit two one-electron oxidations at a platinum disk electrode in dichloromethane separated by approximately 0.5 V at potentials accessible by chemical oxidants. The tetranuclear complexes were selectively oxidized to the 63-electron mixed-valence cationic complexes $[M_4(\mu\text{-PySO})_2(\text{diolefin})_4]^+$ (**1a**$^+$, **2**$^+$, and **3**$^+$) by using $AgCF_3SO_3$ as oxidant and isolated as the triflate salts. Alternatively, the oxidation with $[Cp_2Fe]PF_6$ gives $[Rh_4(\mu\text{-PySO})_2(cod)_4][PF_6]$ (**1b**$^+$). The parameters obtained from the simulation of the electron paramagnetic resonance spectra of the oxidized species strongly suggest that the unpaired electron is delocalized over only two metal atoms in the complexes.

Introduction

Polynuclear transition metal complexes have attracted considerable attention because of their potential chemical reactivity based on a cooperative action of the metal centers and the promising applications as electronic and optoelectronic materials and catalyst.[1] The design of suitable polydentate bridging ligands plays an important role in the construction of polynuclear transition metal complexes to control the structure and more importantly, to impart the necessary flexibility to adapt both to variations of metal−metal separations and to the coordination geometry about

*To whom correspondence should be addressed. E-mail: oro@unizar.es (L.A.O.), perez@unizar.es (J.P.-T.). Fax: +34 976761143.

(1) (a) *The Chemistry of Metal Cluster Complexes*; Shriver, D. F.; Kaesz, H. D., Adams, R. D., Eds.; VCH: New York, 1990. (b) *Metal Clusters in Chemistry*; Braunstein, P., Oro, L. A., Raithby, P. R., Eds.; Wiley-VCH: Weinheim, 1999. (c) *Catalysis by di- and Polynuclear Metal Cluster Complexes*; Adams, R. D., Cotton, F. A., Eds.; Wiley-VCH: New York, 1998.

(2) (a) Higashihara, G.; Inagaki, A.; Akita, M. *Dalton Trans.* **2008**, 1888. (b) Dubs, C.; Yamamoto, T.; Inagaki, A.; Akita, M. *Organometallics* **2006**, *25*, 1344. (c) Dubs, C.; Yamamoto, T.; Inagaki, A.; Akita, M. *Organometallics* **2006**, *25*, 1359. (d) Tanaka, S.; Dubs, C.; Inagaki, A.; Akita, M. *Organometallics* **2005**, *24*, 163. (e) Raper, E. S. *Coord. Chem. Rev.* **1997**, *165*, 475. (f) Balch, A. L. *Prog. Inorg. Chem.* **1994**, *41*, 239.

(3) (a) Berry, J. F. In *Multiple Bonds between Metal Atoms*, 3rd ed.; Cotton, F. A., Murillo, C. A., Walton, R. A., Eds.; Springer-Science and Business Media, Inc.: New-York, 2005. (b) Yeh, C.-Y.; Wang, C.-C.; Chen, C.-h.; Peng, S.-M. In *Nano Redox Sites: Nano-Space Control and its Applications*; Hirao, T., Ed.; Springer: Berlin, 2006; Chapter 5, pp 85−117. (c) Liu, I. P.-C.; Bénard, M.; Hasanov, H.; Chen, I.-W. P.; Tseng, W.-H.; Fu, M.-D.; Rohmer, M.-M.; Chen, C.-h.; Lee, G.-H.; Peng, S.-M. *Chem.—Eur. J.* **2007**, *13*, 8667. (d) Cotton, F. A.; Chao, H.; Murillo, C. A.; Wang, X. *Dalton Trans.* **2006**, 5416. (e) Villarroya, B. E.; Tejel, C.; Rohmer, M. M.; Oro, L. A.; Ciriano, M. A.; Bénard, M. *Inorg. Chem.* **2005**, *44*, 6536. (f) Berry, J. F.; Cotton, F. A.; Murillo, C. A; Roberts, B. K. *Inorg. Chem.* **2004**, *43*, 2277. (g) Tejel, C.; Ciriano, M. A.; Villarroya, B. E.; López, J. A.; Lahoz, F. J.; Oro, L. A. *Angew. Chem., Int. Ed.* **2003**, *42*, 529.

(4) (a) Song, H.-B; Zhang, Z.-Z.; Hui, Z.; Che, C.-M.; Mak, T. C. W. *Inorg. Chem.* **2002**, *41*, 3146. (b) Song, H.-B.; Zhang, Z.-Z.; Mak, T. C. W. *Inorg. Chem.* **2001**, *40*, 5928. (c) Kuang, S.-M.; Zhang, Z.-Z.; Wang, Q.-G.; Mak, T. C. W. *Polyhedron* **1999**, *18*, 493. (d) Marsh, R. E.; Olmstead, M. M.; Schaefer, W. P.; Schomaker, V. *Inorg. Chem.* **1993**, *32*, 4658. (e) Balch, A. L.; Hope, H.; Wood, F. E. *J. Am. Chem. Soc.* **1985**, *107*, 6936. (f) Wood, F. E.; Olmstead, M. M.; Balch, A. L. *J. Am. Chem. Soc.* **1983**, *105*, 6332.

Published on Web 07/16/2009

the metal atoms.[2−5] In this context, oligo-(α-pyridyl)amido ligands represent an outstanding example of ligand design for the synthesis of extended metal atom chains (EMAC).[3] Interestingly, some rigid tridentate ligands based on a 2,6-difunctionalized pyridine scaffold, as, for example, 2,6-bis-(diphenylphosphino)pyridine and 6-diphenylphosphino-2-pyridonate, with a linear disposition of the P, N, P and P, N, O donor atoms set imposed by the rigid pyridine and pyridone frameworks, respectively, have also met success in the stabilization of linear metal arrays.[4,5]

We have been interested for some time in the application of small bite polydentate ligands for the construction of polynuclear complexes.[6] In particular, we have been intensively exploring the potential of polydentate ligands containing sulfur atoms in the donor set like pyridine-2-thiolate, benzothiazole-2-thiolate, or benzimidazole-2-thiolate.[7] This strategy led us to study the coordination chemistry of the doubly thiolate functionalized pyridine ligand 2,6-pyridinedithiolate (PyS_2^{2-}) and the synthesis of $[M_4(\mu\text{-}PyS_2)_4(\text{diolefin})_4]$ (M = Rh, Ir) tetranuclear complexes having an unusual structure that results from the coordination of each tridentate 2,6-pyridinedithiolate ligand to the four d^8 metal centers arranged in a bent-zigzag disposition.[8] This coordination mode produces a tetranuclear framework that contains available coordination donor sites on the peripheral sulfur atoms oriented in a divergent fashion (Scheme 1a).

Scheme 1. Synthesis of Tetranuclear Complexes Directed by 2,6-Dimercaptopyridine (a) and 6-Mercapto-pyridin-2-ol (b)

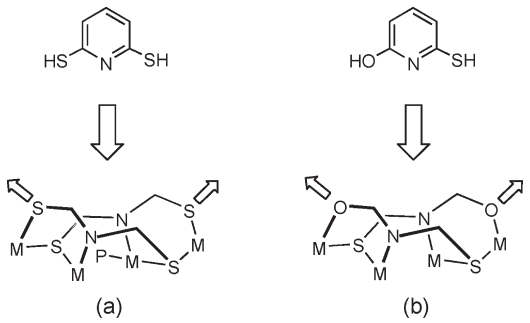

Metal containing building blocks are of particular interest in supramolecular chemistry, and the utilization of molecular complexes as ligands is a well-established methodology for the formation of heterobimetallic extended solids.[9] However, transition-metal clusters and polynuclear complexes are also an attractive class of structural and functional building blocks in supramolecular chemistry.[10] The ability of these tetranuclear complexes to act as *S*,*S* coordination entities have been demonstrated by the assembly of coordination polymers using the complexes $[Rh_4(\mu\text{-}pyS_2)_4(\text{diolefin})_4]$ (diolefin = cod, tfbb) as building blocks. Thus, cationic one-dimensional coordination polymers such as $[AgRh_4(\mu\text{-}PyS_2)_2(\text{diolefin})_4]_n[BF_4]_n$ and $[Rh_5(\mu\text{-}PyS_2)_2(\text{diolefin})_5]_n[BF_4]_n$ resulted from the zigzag chain arrangement of alternating $[Rh_4]$ tetranuclear units and Ag^+ (d^{10}) and $[Rh(\text{diolefin})]^+$ (d^8) metal fragments.[11] In addition, the determination of the structure of the polymer $[ClCuRh_4(\mu\text{-}PyS_2)_4(\text{cod})_4]_n$ has revealed that the self-assembly process of coordination polymers containing trigonal-planar metal fragments as linkers is chiroselective since the one-dimensional chains are formed exclusively by homochiral $[Rh_4]$ building blocks.[12]

The tetranuclear complexes $[M_4(\mu\text{-}PyS_2)_4(\text{cod})_4]$ behave as encapsulating agents for the thallium(I) ion through the formation of cationic pentametallic species $[TlM_4(\mu\text{-}PyS_2)_4(\text{cod})_4]^+$ (M = Rh, Ir) involving a structural reorganization of the molecular framework that makes possible the existence of d^8-s^2-d^8 bonding interactions.[13] Besides, these compounds are redox active and the 63-electron mixed-valence paramagnetic complexes $[M_4(\mu\text{-}PyS_2)_4(\text{cod})_4]^+$ are easily obtained by chemical oxidation of the corresponding tetranuclear complexes using mild one-electron oxidants.[14]

On the basis of this interesting coordination chemistry exhibited by these tetranuclear complexes, we have envisaged the design of tetranuclear *O*,*O* coordination entities as structural motifs for supramolecular chemistry. These new tetranuclear complexes should be accessible from the doubly deprotonated 6-mercaptopyridin-2-ol (H_2PySO) ligand (Scheme 1b).

(5) (a) Mashima, K.; Shimoyama, Y.; Kusumi, Y.; Fukumoto, A.; Yamagata, T.; Ohashi, M. *Eur. J. Inorg. Chem.* **2007**, 235. (b) Ruffer, T.; Ohashi, M.; Shima, A.; Mizomoto, H.; Kaneda, Y.; Mashima, K. *J. Am. Chem. Soc.* **2004**, *126*, 12244. (c) Mashima, K.; Fukumoto, A.; Nakano, H.; Kaneda, Y.; Tani, K.; Nakamura, A. *J. Am. Chem. Soc.* **1998**, *120*, 12151. (d) Mashima, K.; Tanaka, M.; Tani, K.; Nakamura, A.; Takeda, S.; Mori, W.; Yamaguchi, K. *J. Am. Chem. Soc.* **1997**, *119*, 4307. (e) Mashima, K.; Nakano, H.; Nakamura, A. *J. Am. Chem. Soc.* **1996**, *118*, 9083. (f) Mashima, K.; Nakano, H.; Nakamura, A. *J. Am. Chem. Soc.* **1993**, *115*, 11632.

(6) Oro, L. A.; Ciriano, M. A.; Pérez-Torrente, J. J.; Villarroya, B. E. *Coord. Chem. Rev.* **1999**, *193−195*, 941.

(7) (a) Tejel, C.; Villarroya, B. E.; Ciriano, M. A.; Edwards, A. J.; Oro, L. A.; Lanfranchi, M.; Tiripicchio, A.; Tiripicchio-Camellini, M. *Inorg. Chem.* **1998**, *37*, 3954. (b) Tejel, C.; Villarroya, B. E.; Ciriano, M. A.; Oro, L. A.; Lanfranchi, M.; Tiripicchio, A.; Tiripicchio-Camellini, M. *Inorg. Chem.* **1996**, *35*, 4360. (c) Ciriano, M. A.; Pérez-Torrente, J. J.; Lahoz, F. J.; Oro, L. A. *Inorg. Chem.* **1992**, *31*, 969. (d) Ciriano, M. A.; Pérez-Torrente, J. J.; Oro, L. A.; Tiripicchio, A.; Tiripicchio-Camellini, M. *J. Chem. Soc., Dalton Trans.* **1991**, 225. (e) Ciriano, M. A.; Pérez-Torrente, J. J.; Viguri, F.; Lahoz, F. J.; Oro, L. A.; Tiripicchio, A.; Tiripicchio-Camellini, M. *J. Chem. Soc., Dalton Trans.* **1990**, 1493. (f) Ciriano, M. A.; Viguri, F.; Pérez-Torrente, J. J.; Lahoz, F. J.; Oro, L. A.; Tiripicchio, A.; Tiripicchio-Camellini, M. *J. Chem. Soc., Dalton Trans.* **1989**, 25.

(8) Pérez-Torrente, J. J.; Casado, M. A.; Ciriano, M. A.; Lahoz, F. J.; Oro, L. A. *Inorg. Chem.* **1996**, *35*, 1782.

(9) (a) Ni, Z. H.; Zhang, L. F.; Tangoulis, V.; Wernsdorfer, W.; Cui, A. L.; Sato, O.; Kou, H. Z. *Inorg. Chem.* **2007**, *46*, 6029. (b) Tanase, S.; Reedijk, J. *Coord. Chem. Rev.* **2006**, *250*, 2501. (c) Przychodzen, P.; Korzeniak, T.; Podgajny, R.; Sieklucka, B. *Coord. Chem. Rev.* **2006**, *250*, 2234. (d) Sieklucka, B.; Podgajny, R.; Przychodzén, P.; Korzeniak, T. *Coord. Chem. Rev.* **2005**, *249*, 2203. (e) Černák, J.; Orendáč, M.; Potočák, I.; Chomič, J.; Orendáčová, A.; Skorepa, J.; Feher, A. *Coord. Chem. Rev.* **2002**, *224*, 51. (f) Garnovskii, A. D.; Kharisov, B. I.; Blanco, L. M.; Sadimenko, A. P.; Uraev, A. I.; Vasilchenko, I. S.; Garnovskii, D. A. *J. Coord. Chem.* **2002**, *55*, 1119.

(10) (a) Amo-Ochoa, P.; Rodríguez-Tapiador, M. I.; Castillo, O.; Olea, D.; Guijarro, A.; Alexandre, S. S.; Gómez-Herrero, J.; Zamora, F. *Inorg. Chem.* **2006**, *45*, 7642. (b) Song, L.; Li, J.; Lin, P.; Li, Z.; Li, T.; Du, S.; Wu, X. *Inorg. Chem.* **2006**, *45*, 10155. (c) Xu, Q. F.; Chen, J. X.; Zhang, W. H.; Ren, Z. G.; Li, H. X.; Zhang, Y.; Lang, J. P. *Inorg. Chem.* **2006**, *45*, 4055. (d) Welch, E. J.; Long, J. R. *Prog. Inorg. Chem.* **2005**, *54*, 1. (e) Mironov, Y. V.; Naumov, N. G.; Brylev, K. A.; Efremova, O. A.; Fedorov, V. E.; Hegetschweiler, K. *Angew. Chem., Int. Ed.* **2004**, *43*, 1297. (f) Selby, H. D.; Roland, B. K.; Zheng, Z. P. *Acc. Chem. Res.* **2003**, *36*, 933. (g) Selby, H. D.; Roland, B. K.; Zheng, Z. P. *Acc. Chem. Res.* **2003**, *36*, 933. (h) Cotton, F. A.; Lin, C.; Murillo, C. A. *Acc. Chem. Res.* **2001**, *34*, 750. (i) Gabriel, J.-C. P.; Boubekeur, K.; Uriel, S.; Batail, P. *Chem. Rev.* **2001**, *101*, 2037. (j) Toma, H. E.; Araki, K.; Alexiou, A. D. P.; Nikolaou, S.; Dovidauskas, S. *Coord. Chem. Rev.* **2001**, *219−221*, 187. (k) Eddaoudi, M.; Moler, D. B.; Li, H. L.; Chen, B.; Reineke, T. M.; O'Keeffe, M.; Yaghi, O. M. *Acc. Chem. Res.* **2001**, *34*, 319.

(11) Casado, M. A.; Pérez-Torrente, J. J.; Ciriano, M. A.; Lahoz, F. J.; Oro, L. A. *Inorg. Chem.* **2004**, *43*, 1558.

(12) Casado, M. A.; Pérez-Torrente, J. J.; Edwards, A. J.; Oro, L. A.; Ciriano, M. A.; Lahoz, F. J. *CrystEngComm.* **2000**, 23.

(13) Casado, M. A.; Pérez-Torrente, J. J.; López, J. A.; Ciriano, M. A.; Lahoz, F. J.; Oro, L. A. *Inorg. Chem.* **1999**, *38*, 2482.

(14) Casado, M. A.; Pérez-Torrente, J. J.; López, J. A.; Ciriano, M. A.; Alonso, P. J.; Lahoz, F. J.; Oro, L. A. *Inorg. Chem.* **2001**, *40*, 4785.

Herein we report on the synthesis of 6-mercaptopyridin-2-ol and their application for the construction of new redox-active $[M_4(\mu\text{-PySO})_2L_4]$ tetranuclear complexes structurally related to $[M_4(\mu\text{-PyS}_2)_4L_4]$ (M = Rh, Ir). In addition, a comparison of the chemical behavior of both types of complexes is described.

Results and Discussion

Synthesis and Properties of 6-Mercapto-pyridin-2-ol. Several mercaptopyridinol derivatives have been described but only the coordination chemistry of 2-mercaptopyridin-3-ol has been investigated.[15] In contrast, the compound 6-mercaptopyridin-2-ol was mentioned but no experimental details were reported.[16] The ligand 6-mercaptopyridin-2-ol has been prepared by reaction of the commercially available 6-chloropyridin-2-ol with a moderate excess of NaSH in refluxing *N*,*N*-dimethylformamide (DMF). The compound was isolated as a hygroscopic pale-yellow solid in good yield and has been fully characterized by HRMS, IR, and NMR.

Although 6-mercaptopyridin-2-ol can be in equilibrium with the amide and thioamide tautomers,[17] namely, 6-mercapto-2(1*H*)-pyridone and 6-hydroxy-2(1*H*)-pyridinethione respectively, the ^{1}H NMR in DMSO-d_6 at room temperature (RT) showed exclusively the presence of the 6-mercapto-2(1*H*)-pyridone tautomer. In addition, the IR spectrum showed several strong absorptions in the region 1650−1530 cm^{-1} that suggests the presence of this tautomer also in the solid state. Interestingly, the compounds 2-mercaptopyridin-3-ol and 3-mercaptopyridin-2-ol also exist mainly as the tautomers 3-hydroxy-2(1*H*)-pyridinethione[18] and 3-mercapto-2(1*H*)-pyridone,[19] respectively.

Synthesis and Characterization of Tetranuclear Diolefin Complexes. The reaction of 6-mercaptopyridin-2-ol (H_2PySO) with two molar-equiv of a solution of KOH in methanol gave a pale yellow solution of the salt K_2PySO. Further reaction with a dichloromethane solution of complex $[Rh(\mu\text{-Cl})(cod)]_2$ gave an orange-red suspension of the tetranuclear complex $[Rh_4(\mu\text{-PySO})_2(cod)_4]$ (**1**) and KCl as byproduct (Scheme 2). Complex **1** was isolated as a red microcrystalline solid in high yield after the separation of the KCl by extraction of the crude with dichloromethane.

The tetranuclear formulation of **1** is supported by the FAB+ mass spectrum in which the molecular ion was observed at *m*/*z* 1094 (100%). The aromatic region of the ^{1}H NMR spectrum showed three characteristic resonances (d, dd and d) for the aromatic protons of both $PySO^{2-}$ ligands. In addition, the olefinic protons and carbons (=CH) of the four cod ligands were observed as eight resonances in the ^{1}H and ^{13}C{^{1}H} NMR spectra in $CDCl_3$. These data indicate the chemical equivalence of both $PySO^{2-}$ ligands and the presence of two types of diolefin ligands, facts that are compatible with the existence of a C_2 axis in the molecule.

Scheme 2. Synthesis of Rhodium Diolefin Complexes $[Rh_4(\mu\text{-PySO})_2(diolefin)_4]$, Carbonylation, and Replacement Reactions

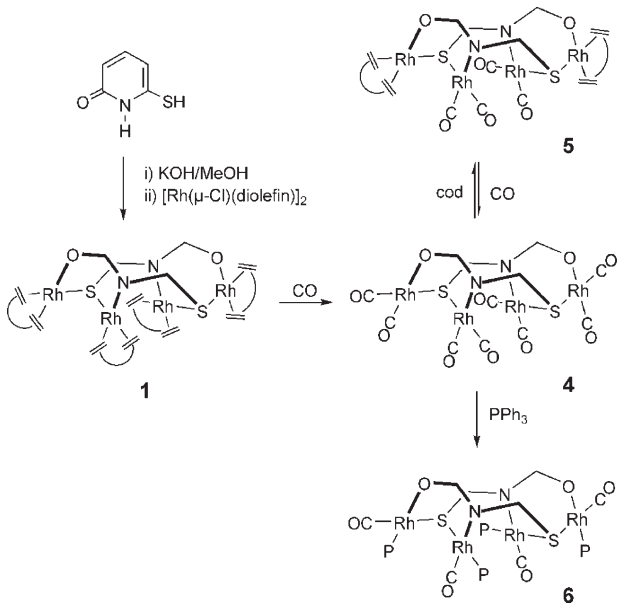

The related diolefin complexes $[Rh_4(\mu\text{-PySO})_2(tfbb)_4]$ (**2**) and $[Ir_4(\mu\text{-PySO})_2(cod)_4]$ (**3**) were obtained as purple and green microcrystalline solids, respectively, in good yield following a similar synthetic procedure. The tetranuclear formulation of the complexes is supported by the microanalysis data and the FAB mass spectra, which showed the molecular ions at the expected values of *m*/*z* (1566 and 1452, respectively). In addition, the NMR data strongly suggest that **1**−**3** are isostructural. In particular, the two $PySO^{2-}$ ligands were found to be equivalent and two types of diolefin ligands were observed both in the ^{1}H and ^{13}C{^{1}H} NMR spectra, in agreement with structures with C_2 symmetry.

Assuming that the tetranuclear complexes $[M_4(\mu\text{-PySO})_2(diolefin)_4]$ and $[M_4(\mu\text{-PyS}_2)_2(diolefin)_4]$ (M = Rh, Ir) are isostructural, there are for the former complex two different coordination modes possible for the *S*,*N*,*O*-tridentate $PySO^{2-}$ ligands that would result in tetranuclear structures of C_2 symmetry: the 1κO, 2κN, 3:4$\kappa^2 S$ coordination mode that produces tetranuclear complexes having oxygen atoms on the periphery, and the less probable 1κS, 2κN, 3:4$\kappa^2 O$ that involve an oxygen atom coordinated in a μ_2 fashion. To establish the coordination mode of the bridging ligands in the tetranuclear complexes, the molecular structure of complex **1** has been studied by X-ray diffraction methods.

Molecular Structure of $[Rh_4(\mu\text{-PySO})_2(cod)_4]$ (1). The molecular framework of the compound consists of four rhodium atoms, arranged in a zigzag chain disposition, supported by two *S*,*N*,*O*-tridentate doubly deprotonated 6-mercaptopyridin-2-ol ligands acting as six electron donors (Figure 1). The molecule exhibits a crystallographic imposed C_2 symmetry, with two "$Rh_2(\mu\text{-PySO})(cod)_2$" moieties forming the tetranuclear complex. Each mercaptopyridinol ligand is bridging two rhodium atoms

(15) (a) Reynolds, J. G.; Sendlinger, S. C.; Murray, A. M.; Huffman, J. C.; Christou, G. *Inorg. Chem.* **1995**, *34*, 5745. (b) Bodini, M. E.; Estefo, C.; Del Valle, M. A. *Polyhedron* **1992**, *11*, 2203. (c) Wen, T. B.; Shi, J. C.; Huang, X.; Chen, Z. N.; Liu, Q. T.; Kang, B. S. *Polyhedron* **1988**, *17*, 331. (d) Howlin, B.; Hider, R. C.; Silver, J. *J. Chem. Soc., Dalton Trans.* **1982**, 1433.

(16) Sasaki, H.; Watanabe, H. Fuji Photo Film Co., Ltd., Japan Patent JP 9211811, **1997**.

(17) (a) Moran, D.; Sukcharoenphon, K.; Puchta, R.; Schaefer, H. F., III; Schleyer, P. V.; Hoff, C. D. *J. Org. Chem.* **2002**, *67*, 9061. (b) Wong, M. W.; Wiberg, K. B.; Frish, M. J. *J. Am. Chem. Soc.* **1992**, *114*, 1645.

(18) Sato, N.; Nagano, E. *J. Heterocyclic Chem.* **1993**, *30*, 691.

(19) Smith, K.; Anderson, D.; Matthews, I. *J. Org. Chem.* **1996**, *61*, 662.

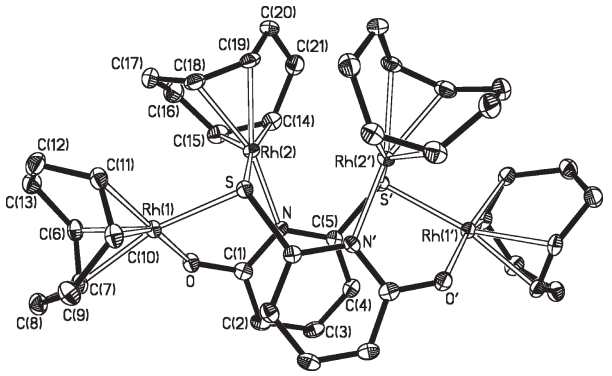

Figure 1. Molecular structure of compound $[Rh_4(\mu\text{-PySO})_2(cod)_4]$ (**1**). Selected bond distances (Å) and angles (deg): Rh(1)−S 2.3890(10), Rh(1)−O 2.110(3), Rh(1)−C(6) 2.129(4), Rh(1)−C(7) 2.138(4), Rh(1)−C(10) 2.085(4), Rh(1)−C(11) 2.093(4), Rh(2)−S 2.3716(10), Rh(2)−N 2.093(3), Rh(2)−C(14) 2.139(4), Rh(2)−C(15) 2.134(4), Rh(2)−C(18) 2.137(4), Rh(2)−C(19) 2.142(4); S−Rh(1)−O 96.86(8), S−Rh(2)−N 86.97(9), S−Rh(1)−M(1) 176.65(11), S−Rh(2)−M(3) 170.53(13), S−Rh(1)−M(2) 90.07(12), S−Rh(2)−M(4) 94.4(6), O−Rh(1)−M(1) 85.26(13), N−Rh(2)−M(3) 91.28(14), O−Rh(1)−M(2) 170.59(13), N−Rh(2)−M(4) 178.6(8), Rh(1)−S−Rh(2) 83.52(3), Rh(1)−O−C(1) 128.2(2) (M labels represent the midpoints of the olefinic bonds).

through the pyridinic nitrogen and oxygen donor atoms ($1\kappa O$, $2\kappa N$) and connecting the other two metals through a sulfur atom coordinated in a μ_2 fashion ($3{:}4\kappa^2 S$).

All the rhodium atoms exhibit slightly distorted square-planar environments resulting from their coordination to two donor atoms of different bridging ligands and a cod molecule chelated through the two olefinic bonds. In agreement with the spectroscopic information obtained in solution, the solid state structure displays two different metal co-ordinations: the external rhodium centers, which are bonded to sulfur and to an oxygen atom, and the internal ones, which are linked to nitrogen and sulfur donor atoms. The differences of these two metal coordination spheres are slightly evidenced in the dissimilar Rh−S bond distances, 2.3890(10) Å and 2.3716(11) Å, but markedly in the bonding of the olefin *trans* to the oxygen of the bridging ligand (Rh-midpoint distances 1.969(4) vs 2.021(3) Å).

The whole tetranuclear molecule closely resembles the related 2,6-pyridinedithiolate analogue, $[Rh_4(\mu\text{-PyS}_2)_2(cod)_4]$.[8] As in this previous structure, the external intermetallic Rh(1)···Rh(2) separation is the shortest one, 3.1708(5) Å, being very similar to that reported in the dithiolate complex, 3.1435(5) Å; however, with no apparent reason, the internal Rh(2)···Rh(2′) distance is markedly shorter in **1**, 3.5028(5) Å, than in the dithiolate analogue, 3.9210(6) Å.[8] Within the metal core the torsion angle Rh(1)−Rh(2)−Rh(2′)−Rh(1′) is 108.11(1)°, while in the dithiolate complex this parameter becomes 125.84(1)°.

The exocyclic C(5)−S distance, 1.777(4) Å, comparable to those observed for the μ^2-*S* atoms in $[Rh_4(\mu\text{-PyS}_2)_2(cod)_4]$, 1.789(4) Å,[8] and in the hexanuclear structurally related $[(PPh_3)_2Au_2)Rh_4(\mu\text{-PyS}_2)_2(tfbb)_4]$ complex, 1.757(10) and 1.790(10) Å,[11] is slightly shorter than typical C−S single bonds (1.83(3) Å in alkanethiolates,[20] for instance) and indicative of the thiolate character of these sulfur atoms. On the other hand, the exocyclic C−O distances of 1.299(5) Å suggest weak electron delocalization of the oxygen lone pairs into the aromatic ring.

Synthesis and Characterization of Rhodium Tetranuclear Carbonyl Complexes. The reaction of complex $[Rh_4(\mu\text{-PySO})_2(cod)_4]$ (**1**) with carbon monoxide under atmospheric pressure in dichloromethane gave an air-sensitive deep violet solution of complex $[Rh_4(\mu\text{-PySO})_2(CO)_8]$ (**4**) (Scheme 2). However, the isolation of **4** from this solution was not possible because of the interference of the replaced cod in the reaction media. An alternative synthetic approach is the reaction of the salt K_2PySO with the dinuclear complex $[Rh(\mu\text{-Cl})(CO)_2]_2$ under a carbon monoxide atmosphere. The compound was isolated as fairly stable violet microcrystals after the separation of the KCl byproduct.

The FAB+ spectrum of compound **4** showed the molecular ion at *m*/*z* 885 with additional peaks resulting from the sequential loss of all the carbonyl ligands, which confirms that the nuclearity is maintained upon carbonylation. The available spectroscopic data indicate that **4** also has C_2 symmetry indicating that its structure is identical to those of the parent diolefin complex replacing each diolefin ligand by two carbonyl groups. Thus, in the $^{13}C\{^1H\}$ NMR spectrum the expected four resonances for the terminal carbonyl ligands (J_{Rh-C} = 72−76 Hz) were observed between δ 185−180 ppm. The aromatic protons of the equivalent $PySO^{2-}$ ligands showed two resonances at δ 6.82 and 5.98 (dd) ppm (2:1 ratio) in $CDCl_3$. The complexity of the resonance at δ 6.82 ppm is a consequence of second order effects, and standard coupling constants were obtained from the simulated spectrum (see Experimental Section).

We have found that the carbonylation of complex $[Rh_4(\mu\text{-PySO})_2(cod)_4]$ (**1**) is partially reversible. When a freshly prepared dichloromethane solution of complex **4**, obtained from the carbonylation of complex **1**, was stirred under argon a deep blue solution of complex $[Rh_4(\mu\text{-PySO})_2(cod)_2(CO)_4]$ (**5**) was obtained. The formation of **5** is a consequence of the replacement of four carbonyl ligands by two molecules of cod in **4**. Obviously, complex **4** can also be obtained by carbonylation of **5** (Scheme 2). The tetranuclear formulation of compound **5** relies on the FAB+ mass spectrum, were the molecular ion was observed at *m*/*z* 990. Although **5** can exist as four different isomers resulting from the location of the cod and carbonyl ligands in the molecular framework, the compound is obtained as a single isomer having C_2 symmetry. Thus, equivalent $PySO^{2-}$ and cod ligands were observed both in ^1H and $^{13}C\{^1H\}$ NMR spectra, whereas the four carbonyl ligands exhibited two doublets at δ 187.6 (J_{Rh-C} = 64 Hz) and 184.7 ppm (J_{Rh-C} = 71 Hz) in the $^{13}C\{^1H\}$ NMR spectrum in $CDCl_3$.

The two structures compatible with the spectroscopic data are shown in Figure 2. Unfortunately, neither the magnitude of the J_{Rh-C} coupling constant nor the chemical shifts of the olefinic resonances (δ 4.98, 4.85, 4.28, and 3.27 ppm) are fully reliable parameters to make a precise structural assignment. However, the pattern of resonances compares well with that observed for the cod ligands coordinated to the outer rhodium atoms in the complex $[Ir_4(\mu\text{-PyS}_2)_2(cod)_4]$, if the shielding effect induced by the O atom *trans* to one of the C=C bonds is

(20) Orpen, A. G.; Brammer, L.; Allen, F. H.; Kennard, O.; Watson, D.; Taylor, R. *J. Chem. Soc., Dalton Trans.* **1991**, S1.

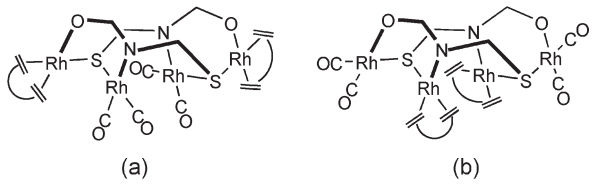

Figure 2. Possible C_2 isomers of compound $[Rh_4(\mu\text{-}PySO)_2(cod)_2(CO)_4]$ (**5**).

taken into consideration.[21] The proposed structure (Figure 2a) is probably also the preferred on steric grounds as the cod ligands are located further apart into the tetranuclear framework.

The reaction of $[Rh_4(\mu\text{-}PySO)_2(CO)_8]$ (**4**), obtained by carbonylation of complex **1** in dichloromethane, with four molar-equiv of triphenylphosphine gave the compound $[Rh_4(\mu\text{-}PySO)_2(CO)_4(PPh_3)_4]$ (**6**) which was isolated as an air-sensitive violet solid in good yield (Scheme 2). Compound **6** can be alternatively prepared by reaction of *trans*-$[RhCl(CO)(PPh_3)_2]$ with the salt K_2PySO (2:1 molar ratio). The spectroscopic data for **6** indicate than the compound is tetranuclear and exists as a single isomer with C_2 symmetry. The molecular ion was observed in the FAB+ mass spectrum at m/z 1822, and the broad band at 1982 cm^{-1} in the IR spectrum evidenced that each rhodium center is coordinated both to a carbonyl and a triphenylphosphine ligand. The $^{31}P\{^1H\}$ NMR spectrum of **6** consisted of two doublets at δ 39.76 and 38.69 ppm (J_{Rh-P} = 163 and 175 Hz, respectively) as expected for a C_2 symmetry. The proposed structure for complex **6** is shown in Scheme 2 and is based on the electronic and steric effects influencing the substitution processes. In particular, the replacement of the carbonyl ligands *trans* to the sulfur atoms in the two inner rhodium centers is driven by the *trans* effect of the sulfur atom[22] and is in agreement with the substitution pattern found in related dinuclear complexes having short-bite *N*,*S* bidentate ligands.[23] However, the values of the observed J_{Rh-P} coupling constants strongly suggest that the substitution on the external rhodium atoms takes place *trans* to the oxygen atoms. Typical values of J_{Rh-P} for P *trans* to S in mono- or dinuclear Rh(I) complexes are around 160 Hz[7f,8,23a] whereas the J_{Rh-P} for P *trans* to O are 175 Hz.[24] This proposal is also supported by steric considerations since the substitution *trans* to the oxygen atoms place further apart the PPh_3 ligands on neighboring rhodium atoms.

Electrochemical Properties of the Tetranuclear Diolefin Complexes. The electrochemical behavior of complexes **1**−**3** and **5** is similar to that exhibited by the tetranuclear complexes supported by 2,6-pyridinedithiolato ligands. The cyclic voltammograms (CV) of the complexes recorded in dichloromethane at 100 mV s^{-1} showed two chemically reversible one-electron charge transfers that can be assigned to the electrogeneration of the mono $[M_4(\mu\text{-}PySO)_2(diolefin)_4]^+$ and dicationic $[M_4(\mu\text{-}PySO)_2(diolefin)_4]^{2+}$ (M = Rh, Ir) species, respectively. The formal electrode potentials ($E°$) for the processes $[M_4] \rightarrow [M_4]^+$ and $[M_4]^+ \rightarrow [M_4]^{2+}$ are shown in Table 1. In addition, the complexes **1** and **3** displayed one additional irreversible anodic process at 1.18 and 1.17 V, respectively. The analysis of both waves in complex $[Rh_4(\mu\text{-}PySO)_2(cod)_4]$ (**1**) with scan rates varying from 0.05 to 0.20 V s^{-1} was indicative of their reversible character.[25] However, the ΔEp of both waves in **2**, **3**, and **5** increased by 20−30 mV when the scan rate was increased from 0.05 to 0.20 V s^{-1}, which is a diagnostic of an electronically quasi-reversible one-electron redox processes.[26]

Table 1. Redox Potentials ($E°$ vs SCE, in V) and Peak-to-Peak Separation (ΔEp in mV) for Complexes $[M_4(\mu\text{-}PySO)_2(diolefin)_4]$ and $[M_4(\mu\text{-}PyS_2)_2(diolefin)_4]$[8] in 0.1 M TBAH/$CH_2Cl_2$ at 100 mV s^{-1}

	$[M_4] \rightarrow [M_4]^+$		$[M_4]^+ \rightarrow [M_4]^{2+}$	
compound	$E°$ (V)	ΔEp (mV)	$E°$ (V)	ΔEp (mV)
$[Rh_4(\mu\text{-}PySO)_2(cod)_4]$ (**1**)	0.25	78	0.77	84
$[Rh_4(\mu\text{-}PySO)_2(tfbb)_4]$ (**2**)	0.49	100	0.84	110
$[Ir_4(\mu\text{-}PySO)_2(cod)_4]$ (**3**)	0.12	105	0.64	102
$[Rh_4(\mu\text{-}PySO)_2(cod)_2(CO)_4]$ (**5**)	0.41	95	0.90	105
$[Rh_4(\mu\text{-}pyS_2)_2(cod)_4]$	0.16	63	0.58	70
$[Rh_4(\mu\text{-}pyS_2)_2(tfb)_4]$	0.37	80	0.79	80
$[Ir_4(\mu\text{-}pyS_2)_2(cod)_4]$	0.08	79	0.53	80

The formal electrode potentials are strongly dependent on the nature of both the metallic center and the auxiliary ligands. Thus, the formal electrode potentials in complex $[Rh_4(\mu\text{-}PySO)_2(tfbb)_4]$ (**2**) were anodically shifted 240 and 70 mV from those observed for $[Rh_4(\mu\text{-}PySO)_2(cod)_4]$ (**1**) which is in agreement with a reduction of the electronic density on the rhodium atoms because of the greater electron-withdrawing character of the tfbb ligands. This effect was also observed in complex $[Rh_4(\mu\text{-}PySO)_2(cod)_2(CO)_4]$ (**5**) which exhibites oxidation waves anodically shifted 160 and 130 mV with reference to those of compound **1**, a fact that is fully consistent with the presence of four π-acid carbonyl ligands. Both oxidation waves in compound $[Ir_4(\mu\text{-}PySO)_2(cod)_4]$ (**3**) are cathodically shifted 130 mV compared with those of compound **1** as expected for the easiest oxidation of the iridium centers.[27] Interestingly, similar trends have been observed along the series of complexes $[M_4(\mu\text{-}PyS_2)_2(diolefin)_4]$ (M = Rh, Ir; diolef = cod, tfbb) although as can be observed in Table 1, in general, the complexes $[M_4(\mu\text{-}PySO)_2(diolefin)_4]$ were found harder to oxidize. The larger differences in the formal electrode potentials, 90 and 190 mV, were observed between complex **1** and $[Rh_4(\mu\text{-}PyS_2)_2(cod)_4]$. This observation can be rationalized by the superior donor ability of sulfur versus oxygen that facilitates the elimination of electrons from the metal centers.

(21) Rodman, G. S.; Mann, K. R. *Inorg. Chem.* **1988**, *27*, 338.
(22) Botha, L. J.; Basson, S. S.; Leipoldt, J. G. *Inorg. Chim. Acta* **1987**, *126*, 25.
(23) (a) Ciriano, M. A.; Pérez-Torrente, J. J.; Lahoz, F. J.; Oro, L. A. *J. Organomet. Chem.* **1993**, *455*, 225. (b) Claver, C.; Kalck, P.; Ridmy, M.; Thorez, A.; Oro, L. A.; Pinillos, M. T.; Apreda, M. C.; Cano, F. H.; Foces-Foces, C. *J. Chem. Soc., Dalton Trans.* **1988**, 1523.
(24) (a) Conradie, J.; Lamprecht, G. J.; Otto, S.; Swarts, J. C. *Inorg. Chim. Acta* **2002**, *328*, 191. (b) Purcell, W.; Basson, S. S.; Leipoldt, J. G.; Roodt, A; Preston, H. *Inorg. Chim. Acta* **1995**, *234*, 153. (c) Trzeciak, A. M.; Ziolkowski, J. J. *J. Organomet. Chem.* **1992**, *429*, 239.
(25) (a) Brown, E. R.; Sandifer, J. R. In *Physical Methods of Chemistry: Electrochemical Methods*; Rossiter, B.W., Hamilton, J. F., Eds.; Wiley: New York, 1986; Vol. *2*. (b) Piraino, P.; Bruno, G.; Tresoldi, G.; Lo Schiavo, S.; Zanello, P. *Inorg. Chem.* **1987**, *26*, 91.
(26) Geiger, W. E., Jr. *Prog. Inorg. Chem.* **1985**, *23*, 275.
(27) (a) Connelly, N. G.; Garcia, G. *J. Chem. Soc., Dalton Trans.* **1987**, 2737. (b) Connelly, N. G.; Garcia, G.; Gilbert, M.; Stirling, J. S. *J. Chem. Soc., Dalton Trans.* **1987**, 1403.

Interestingly the two reversible one-electron processes in the $[M_4(\mu\text{-PySO})_2(\text{diolefin})_4]$ complexes occur at formal electrode potentials that are accessible by chemical reagents. In addition, the large difference between the formal potentials of both oxidation processes (350−520 mV) ensures that the $[M_4]^+$ species should be stable with respect to disproportionation into the $[M_4]$ and $[M_4]^{2+}$ complexes. In fact, the calculated K_{disp} values for the disproportionation equilibria are in the range $10^{-6}-10^{-9}$.[28]

Synthesis of Paramagnetic Tetranuclear Complexes by Chemical Oxidation. The oxidation of the tetranuclear complexes with mild one-electron oxidants resulted in the formation of cationic 63-electron mixed-valence paramagnetic complexes $[M_4(\mu\text{-PySO})_2(\text{diolefin})_4]^+$. The reaction of complexes $[M_4(\mu\text{-PySO})_2(\text{diolefin})_4]$ (**1**−**3**) with one molar equiv of $AgCF_3SO_3$ in dichloromethane gave the cationic complexes $[Rh_4(\mu\text{-PySO})_2(cod)_4][CF_3SO_3]$ (**1a**$^+$), $[Rh_4(\mu\text{-PySO})_2(tfbb)_4][CF_3SO_3]$ (**2**$^+$), and $[Ir_4(\mu\text{-PySO})_2(cod)_4][CF_3SO_3]$ (**3**$^+$) which were isolated as deep colored microcrystalline solids in good yield. Alternatively, compound $[Rh_4(\mu\text{-PySO})_2(cod)_4][PF_6]$ (**1b**$^+$) can be obtained by reaction of **1** with $[Cp_2Fe]PF_6$ in dichloromethane (1:1 molar ratio).

The paramagnetic complexes **1**$^+$, **2**$^+$, and **3**$^+$ have been characterized by elemental analyses, FAB$^+$, and electron paramagnetic resonance (EPR) spectroscopy. The complexes behave as 1:1 electrolytes in acetone and display the peaks corresponding to molecular ions $[M_4(\mu\text{-PySO})_2(\text{diolefin})_4]^+$ in the FAB$^+$ mass spectra. Furthermore, the formulation of complexes as paramagnetic monooxidized species was established electrochemically by linear voltammetry at RDE.

EPR spectra of polycrystalline samples of **1a**$^+$, **2**$^+$, and **3**$^+$ have been measured in X- and Q-band spectra at RT. The X-band spectra consist of a slightly asymmetric line centered at a *g*-value between 2.1 and 2.3. On the other hand two clearly resolved features appear in the Q-band spectra (see Figures 3 and 4) suggesting that the local symmetry is close to axial. In fact the spectra can be associated to an $S = 1/2$ paramagnetic entity and a slightly orthorhombic *g*-tensor has to be considered. So, for describing them, the following spin-Hamiltonian has been used:

$$H = \mu_B B\{g_x l_x S_x + g_y l_y S_y + g_z l_z S_z\}$$

where μ_B is the Bohr magneton, B is the strength of the applied magnetic field and (l_x, l_y, l_z) are the director cosines that the magnetic field makes with the principal axis of the *g*-tensor whose principal values are g_x, g_y, g_z.

To estimate these values several spectra have been calculated taking a Lorentzian line shape with an anisotropic halfwidth. In this way the values given in Table 2 have been obtained, and the calculated spectra are represented by dotted lines in Figures 3 and 4. The values of the isotropic contribution of the *g*-tensor, $g_0 = (g_x + g_y + g_z)/3$, are also given in Table 2.

It is interesting to note that the g_0 value obtained for **1a**$^+$ and **2**$^+$ (Table 2) was similar to that previously reported for $[Rh_4(\mu\text{-PyS}_2)_2(cod)_4]^+$ ($g_0 = 2.16 \pm 0.01$) and $[Rh_4(\mu\text{-PyS}_2)_2(tfbb)_4]^+$ ($g_0 = 2.11 \pm 0.01$).[14] In particular, when a frozen solution of $[Rh_4(\mu\text{-PyS}_2)_2(cod)_4]^+$ was measured a hyperfine structure corresponding to an interaction with two equivalent ^{103}Rh nuclei was resolved. That was interpreted considering that the unpaired electron was mainly located in two equivalent rhodium centers. The similar value of g_0 strongly suggests that the same occurs in **1a**$^+$. A trickier fact is the different g_0 value in **1a**$^+$ and **2**$^+$, suggesting a higher unpaired electron delocalization when tfbb ligand replaces cod. Although the lack of resolved hyperfine structure in **2**$^+$ as

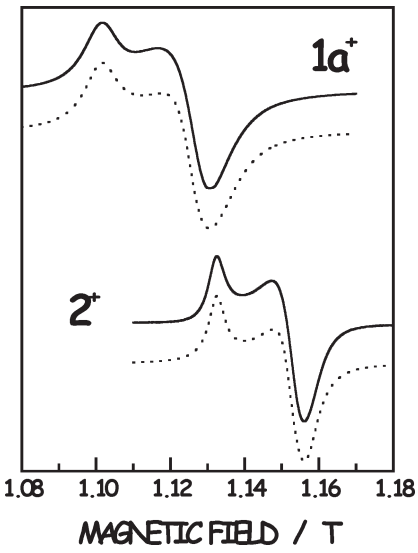

Figure 3. Q-band (34 GHz) EPR spectra of polycrystalline powdered sample of **1a**$^+$ and **2**$^+$. Dotted lines correspond to calculated spectra with the parameters given in Table 2 (see text for details). These last ones have been shifted down a 25% of their whole amplitude.

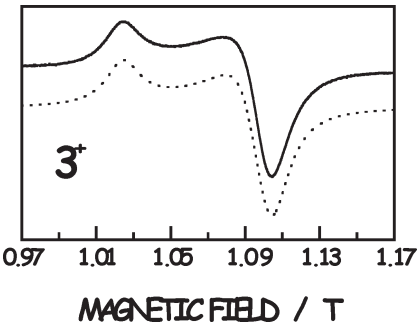

Figure 4. Q-band (34 GHz) EPR spectrum of polycrystalline powdered sample of **3**$^+$. Dotted line corresponds to the calculated spectrum with the parameters given in Table 2 (see text for details). This last one has been shifted down a 25% of its whole amplitude.

Table 2. Principal Values of the *g*-Tensor[a], Isotropic Contribution to the *g*-tensor (g_0), and Halfwidth of the Lorentzian Lineshape used in the Simulation Spectra of the Complexes $[M_4(\mu\text{-PySO})_2(\text{diolefin})_4]^+$

compound	g_x, W_x (mT)	g_y, W_y (mT)	g_z, W_z (mT)	g_0
1a$^+$	2.145, 10.6	2.158, 6.5	2.205, 6.3	2.169
2$^+$	2.100, 5.0	2.108, 4.5	2.145, 3.0	2.118
3$^+$	2.201, 13.0	2.221, 15.0	2.371, 13.0	2.264

[a] The estimated uncertainty in the *g*-values is ± 0.008 in all the cases.

(28) Gagné, R. R.; Spiro, C. L.; Smith, T. J.; Hamann, C. A.; Thies, W. R.; Shiemke, A. K. *J. Am. Chem. Soc.* **1981**, *103*, 4073.

well as in $[Rh_4(\mu\text{-}PyS_2)_2(tfbb)_4]^+$, even in a frozen solution, prevent the determination of the number of metal centers sharing the unpaired electron; the decrease of the g_0 value as compared with that found in $\mathbf{1a}^+$ and $[Rh_4(\mu\text{-}PyS_2)_2(cod)_4]^+$ could be a consequence of the different electron acceptor character of the diolefin ligand, higher in tfbb than in cod. This also can account for the decrease of the *g*-tensor anisotropy.

On the other hand, the observed decrease of the *g*-tensor anisotropy in complexes $[Rh_4(\mu\text{-}PySO)_2(diolefin)_4]^+$ when compared with $[Rh_4(\mu\text{-}PyS_2)_2(diolefin)_4]^+$ could be associated with some structural modification, probably related with the metal−metal separation, driven by the different bridging ligands (μ-PySO and μ-PyS_2) because the g_0 value does not change. In the case of the related iridium tetranuclear compounds, the differences observed between $[Ir_4(\mu\text{-}PyS_2)_2(cod)_4]^+$ and $[Ir_4(\mu\text{-}PySO)_2(cod)_4]^+$ can be explained similarly.

The chemical reversibility associated to the redox processes leading to the oxidized species $[M_4(\mu\text{-}PySO)_2(diolefin)_4]^+$ and $[M_4(\mu\text{-}PySO)_2(diolefin)_4]^{2+}$ suggests that the tetranuclear framework is maintained upon oxidation. Thus, the main structural changes probably affect the metal−metal separations as it has been found in related di- and trinuclear complexes.[29] An extended Hückel molecular orbital calculation carried out on complex $[Rh_4(\mu\text{-}PyS_2)_2(cod)_4]$ showed the antibonding character of the highest occupied molecular orbital (HOMO) in the tetranuclear species, and thus a shortening of the metal−metal distances upon oxidation should be also expected in the complexes $[M_4(\mu\text{-}PySO)_2(diolefin)_4]$. Unfortunately, we have failed to obtain good quality crystals of any of the oxidized species, even using different anions, to confirm this result. In addition, attempts to prepared the dicationic complexes $[M_4(\mu\text{-}PySO)_2(diolefin)_4]^{2+}$ using silver salts as oxidants were unsuccessful.

Coordination Chemistry of the complexes $[M_4(\mu\text{-}pySO)_2L_4]$. The coordination mode of the 6-mercaptopyridin-2-ol ligands in the complexes $[M_4(\mu\text{-}PySO)_2L_4]$ (M = Rh, Ir) produces a tetranuclear framework with two oxygen atoms oriented in a divergent fashion available for coordination (Scheme 1b). Although these complexes are potential *O*,*O* donor entities they have shown weaker coordination ability than the *S*,*S* donor $[M_4(\mu\text{-}PyS_2)_2L_4]$ tetranuclear counterparts, previously reported.[11,12] Thus, the compound $[Rh_4(\mu\text{-}PySO)_2(cod)_4]$ (**1**) failed to react with the species $[Rh(cod)(NCCH_3)_2]BF_4$ that has two labile acetonitrile ligands. However, evidence of a weak interaction between and **1** and Tl^+ was obtained from ^1H NMR data in solution ($CDCl_3$) because a pronounced low field shift (0.22 ppm) of the resonance attributable to the *meta* protons adjacent to the oxygen atoms of the bridgind ligands has been observed.[30]

The reaction of $[Rh_4(\mu\text{-}PySO)_2(cod)_4]$ (**1**) with the solvated species $[Au(PPh_3)(Me_2CO)_X]^+$ in acetone/dichloromethane gave a deep-red solution. The ^1H NMR spectrum of the isolated red-brick solid in $CDCl_3$ at 223 K showed six well-defined resonances of equal intensity for the $PySO^{2-}$ bridging ligands which is compatible with the formation of the pentanuclear cation $[(PPh_3)AuRh_4(\mu\text{-}PySO)_2(cod)_4]^+$ (**7**). However, we observed that compound **1** crystallized out from these solutions which is an indication of the weak coordination of the fragment $[Au(PPh_3)]^+$ to one of the O donor sites in **1**. In contrast, the protonation of complex **1** with CF_3SO_3H in CH_2Cl_2 resulted in the breakdown of the tetranuclear structure and the formation of unidentified species.

Concluding Remarks

We have described the high yield synthesis of rhodium and iridum tetranuclear complexes $[M_4(\mu\text{-}PySO)_2(diolefin)_4]$ (M = Rh, Ir; diolefin = cod, tfbb) from the doubly deprotonated form of the new ligand 6-mercapto-2(1*H*)-pyridone. The C_2 symmetry tetranuclear structure is supported by two *S*,*N*,*O*-tridentate ligands acting as six electron donor ligands. The coordination mode of the ligand determines the formation of the isomer having two peripheral oxygen donor atoms oriented in a divergent fashion. However, both sites have a marginal nucleophilic character and only a weak coordination with selected metal ion fragments has been observed. The tetranuclear complexes are redox-active species that undergo two stepwise one-electron oxidation processes, and the monooxidized mixed-valence paramagnetic tetranuclear species have been prepared by chemical oxidation. Interestingly, the integrity of the rhodium tetranuclear framework is also sustained upon carbonylation, and the carbonyl complex undergoes stereoselective replacement reactions by 1,5-cyclooctadiene and triphenylphosphine ligands.

Experimental Section

General Methods. All manipulations were performed under a dry nitrogen atmosphere using Schlenk-tube techniques. Solvents were dried by standard methods and distilled under argon immediately prior to use. Standard literature procedures were used to prepare the starting materials $[Rh(\mu\text{-}Cl)(diolefin)]_2$ (diolefin = cod,[31] tfbb),[32] $[Ir(\mu\text{-}Cl)(cod)]_2$,[33] $[Rh(\mu\text{-}Cl)(CO)_2]_2$,[34] *trans*-$[RhCl(CO)(PPh_3)_2]$,[35] $[AuCl(PPh_3)]$,[36] and $[Cp_2Fe][PF_6]$.[37] $AgCF_3SO_3$ and 6-chloro-2-pyridinol were purchased from Fluka Chem. and Aldrich, respectively. $NaSH\cdot H_2O$ (Aldrich) was used immediately on delivery.

Physical Measurements. IR spectra were recorded on a Perkin-Elmer FT-IR Spectrum One. Elemental C, H, N, and S analysis were performed in a 240-C Perkin-Elmer microanalyzer. Conductivities were measured in about 5×10^{-4} M acetone solutions using a Philips PW 9501/01 conductimeter. Mass spectra were recorded in a VG Autospec double-focusing mass spectrometer operating in the FAB or EI modes. The ions were produced by the standard Cs^+ gun at about 30 KV; 3-nitrobenzyl alcohol (NBA) was used as matrix. Electrospray mass spectra (ESI-MS) were recorded in methanol on a Bruker MicroTof-Q using sodium formiate as reference. ^1H, $^{13}C\{^1H\}$,

(29) (a) Connelly, N. G.; Hayward, O. D.; Klangsinsirikul, P.; Orpen, A. G.; Rieger, P. H. *Chem. Commun.* **2000**, 963. (b) Villarroya, B. E.; Oro, L. A.; Lahoz, F. J.; Edwards, A. J.; Ciriano, M. A.; Alonso, P. J.; Tiripicchio, A.; Tiripicchio-Camellini, M. *Inorg. Chim. Acta* **1996**, *250*, 241. (c) Boyd, D. C.; Neil, G.; Connelly, N. G.; Garcia Herbosa, G.; Hill, M. G.; Mann, K. R.; Mealli, C.; Orpen, A. G.; Richardson, K. E.; Rieger, P. H. *Inorg. Chem.* **1994**, *33*, 960.
(30) (a) Isab, A. A.; Wazeer, M. I. M. *Spectrochim. Acta A* **2006**, *65*, 191. (b) Alizadeh, N.; Bordbar, M.; Shamsipur, M. *Bull. Chem. Soc. Jpn.* **2005**, *78*, 1763.
(31) Giordano, G.; Crabtree, R. H. *Inorg. Synth.* **1979**, *19*, 218.
(32) Roe, D. E.; Masey, A. G. *J. Organomet. Chem.* **1979**, *28*, 273.
(33) Herde, J. L.; Lambert, J. C.; Senoff, C. V. *Inorg. Synth.* **1974**, *15*, 18.
(34) Powel, J.; Shaw, B. L. *J. Chem. Soc., Dalton Trans.* **1968**, 211.
(35) Bonati, F.; Wilkimson, G. *J. Chem. Soc.* **1964**, 3155.
(36) Braunstein, P.; Lehner, H.; Matt, D. *Inorg. Synth.* **1990**, *27*, 218.
(37) Smart, J. C.; Pinsky, B. L. *J. Am. Chem. Soc.* **1980**, *102*, 1009.

and $^{31}P\{^{1}H\}$ NMR spectra were recorded on a Varian Gemini 300 spectrometer operating at 300.08, 75.46, and 121.47 MHz respectively. Chemical shifts are reported in ppm and referenced to $SiMe_4$ using the residual resonances of the deuterated solvents (^{1}H and ^{13}C) and 85% H_3PO_4 (^{31}P) as external reference respectively. Assignments in complex NMR spectra were done by simulation with the program gNMR v 3.6 (Cherwell Scientific Publishing Limited) for Macintosh. EPR spectra were measured in a Bruker ESP380E spectrometer working either in X-band (≈9.5 GHz) or Q-band (≈34 GHz). Powdered polycrystalline samples were introduced in standard EPR quartz tubes, and the spectra were run at RT. The magnetic field was measured with a Bruker ER035 M NMR gaussmeter, and a 5350B HP frequency counter was used for determining the microwave frequency. Cyclic voltammetric experiments were performed with an EG&G PARC Model 273 potentiostat/galvanostat using a three-electrode glass cell consisting of a platinum-disk working electrode, a platinum-wire auxiliary electrode, and a standard calomel reference electrode (SCE). Linear voltamperometry was performed using a rotating platinum electrode (RDE) as the working electrode. Tetra-*n*-butylammoniumhexafluorophosphate (TBAH) was employed as supporting electrolyte. Electrochemical experiments were carried out under nitrogen in about 5×10^{-4} M dichloromethane solutions of the complexes and 0.1 M in TBAH. The $[Fe(C_5H_5)_2]^{+}/[Fe(C_5H_5)_2]$ couple is observed at +0.47 V under these experimental conditions.

Synthesis of 6-Mercaptopyridin-2-ol (H_2PySO). $NaSH \cdot H_2O$ (8.50 g, 0.115 mol) was dissolved in refluxing DMF (90 mL) under argon. After cooling, a solution of 6-chloropyiridin-2-ol (5.0 g, 0.038 mol) in dimethylformamide (10 mL) was added, and the solution heated for 16 h at 418 K. The mixture was cooled, and the precipitated salt was filtered off to obtain an orange-brown solution. The solvent was mostly removed by distillation under vacuum, and the oily brown residue dissolved in 40 mL of a methanol-THF mixture (1:3). The solution was filtered through Celite, and the resulting orange solution brought to dryness under vacuum. The residue was stirred with diethylether to give a cream solid that was filtered, washed with diethylether, and dried under vacuum. The solid was dissolved in the minimum amount of a dichlorometane-methanol mixture (4:1) and then eluted through a silica gel column using dichlorometane/methanol (2:1). The eluted orange solution was brought to dryness under vacuum, and the residue stirred in tetrahydrofuran (THF). Slow addition of diethyl ether gave the compound as a hygroscopic pale-yellow solid that was filtered, washed with diethyl ether, and dried under vacuum. Yield 3.650 g (74%). ^{1}H NMR (DMSO-d_6, 293 K) δ: 10.56 (br, NH), 6.96 (dd, J_{H-H} = 8.4 Hz, J_{H-H} = 7.2 Hz), 5.96 (d, J_{H-H} = 7.2 Hz), 5.51 (d, J_{H-H} = 8.4 Hz), 3.51 (br, SH). $^{13}C\{^{1}H\}$ NMR (DMSO-d_6, 293 K) δ: 169.8 (C=O), 164.6 (C-S), 140.1, 109.0, 103.5. IR (cm^{-1}): 3300−2400 (br, SH, NH), 1648, 1601, 1537. MS (EI, CH_3OH, *m*/*z*): 127 (H_2pySO, 100%), 94 (HpyO, 20%). HRMS calcd for C_5H_6NOS 128.01646, found 128.01652.

Synthesis of the Complexes. [Rh_4(μ-PySO)$_2$(cod)$_4$] (1). H_2PySO (0.052 g, 0.406 mmol) was reacted with a solution of KOH in methanol (2.91 mL, 0.278 M, 0.811 mmol) in methanol (5 mL) to give a pale-yellow solution of K_2PySO. This solution was further reacted with a solution of [Rh(μ-Cl)(cod)]$_2$ (0.200 g, 0.406 mmol) in dichloromethane (10 mL) to give an orange suspension after stirring for 12 h. The solvent was removed under vacuum, and the residue dissolved in dichloromethane (25 mL) and then filtered through Celite. Concentration of this solution to about 1 mL and slow addition of methanol afforded the compound as a red-orange microcrystalline solid which was collected by filtration, washed with methanol, and dried under vacuum. Yield: 0.200 g (90%). Anal. Calcd for $C_{42}H_{54}N_2O_2Rh_4S_2$: C, 46.08; H, 4.97; N, 2.56; S, 5.86. Found: C, 46.43; H, 4.63; N, 2.67; S, 5.93. MS (FAB^{+}, CH_2Cl_2, *m*/*z*): 1094 (M^{+}, 100%), 986 (M^{+} − cod, 10%), 878 (M^{+} − 2cod, 7%). Mol. Weight ($CHCl_3$). Found: 1065 (Calcd. 1094). ^{1}H NMR ($CDCl_3$, 293 K) δ: 7.76 (d, 2H, J_{H-H} = 7.1 Hz), 6.77 (dd, 2H, J_{H-H} = 8.7 Hz, J_{H-H} = 7.1 Hz), 5.74 (d, 2H, J_{H-H} = 8.7 Hz) (pySO); 4.95 (m, 2H, =CH), 4.89 (m, 2H, =CH), 4.79 (m, 2H, =CH), 4.75 (m, 2H, =CH), 4.14 (m, 2H, =CH), 3.95 (m, 2H, =CH), 3.91 (m, 2H, =CH), 3.38 (m, 2H, >CH$_2$), 3.31 (m, 2H, =CH), 2.80−2.35 (m, 14H, >CH$_2$), 2.22 (m, 2H, >CH$_2$), 2.05 (m, 2H, >CH$_2$) 1.94 (m, 6H, >CH$_2$), 1.76 (m, 6H, >CH$_2$) (cod). $^{13}C\{^{1}H\}$ NMR ($CDCl_3$, 293 K) δ: 170.7 (C-O), 161.6 (C-S), 137.9, 117.2, 111.9 (CH) (pySO); 91.3 (d, J_{Rh-C} = 12 Hz), 88.0 (d, J_{Rh-C} 12 Hz), 82.9 (d, J_{Rh-C} 13 Hz), 81.3 (d, J_{Rh-C} = 11 Hz), 79.0 (d, J_{Rh-C} = 12 Hz), 76.7 (d, J_{Rh-C} = 12 Hz), 68.9 (d, J_{Rh-C} = 14 Hz), 67.2 (d, J_{Rh-C} = 15 Hz) (=CH, cod); 34.2, 32.5, 31.3, 30.9, 30.4, 30.2, 30.6, 28.8 (>CH$_2$, cod).

[Rh_4(μ-PySO)$_2$(tfbb)$_4$] (2). To a solution of K_2PySO (0.274 mmol) in methanol (5 mL), obtained by reaction of H_2PySO with a solution of KOH in methanol, was added a solution of [Rh(μ-Cl)(tfbb)]$_2$ (0.200 g, 0.274 mmol) in dichloromethane (10 mL). The mixture was reacted for 12 h to give a purple suspension. Work-up as described above gave the compound as a purple microcrystalline solid. Yield: 0.183 g (85%). Anal. Calcd for $C_{58}H_{30}F_{16}N_2O_2Rh_4S_2$: C, 44.47; H, 1.93; N, 1.79; S, 4.09. Found: C, 44.51; H, 1.83; N, 1.73; S, 4.18. MS (FAB^{+}, CH_2Cl_2, *m*/*z*): 1566 (M^{+}, 100%), 1340 (M^{+} − tfbb, 6%), 1237 (M^{+} − Rh(tfbb), 4%), 1114 (M^{+} − 2tfbb, 11%), 888 (M^{+} − 3tfbb, 6%), 784 (M^{+} − 2Rh(tfbb) − pySO, 40%). ^{1}H NMR ($CDCl_3$, 293 K) δ: 7.38 (d, 2H, J_{H-H} = 6.9 Hz), 6.82 (dd, 2H, J_{H-H} = 8.5 Hz, J_{H-H} = 6.9) (pySO); 6.40 (m, 2H, CH), 5.84 (m, 4H, CH) (tfbb), 5.79 (d, 2H, J_{H-H} = 8.5) (pySO), 5.50 (m, 2H, CH), 5.34 (m, 2H, =CH), 4.66 (m, 2H, =CH), 4.50 (m, 2H, =CH), 4.34 (m, 2H, =CH), 3.98 (m, 2H, =CH), 3.84 (m, 4H, =CH), 2.97 (m, 2H, =CH) (tfbb).

[Ir_4(μ-PySO)$_2$(cod)$_4$] (3). K_2PySO (0.223 mmol) and [Ir(μ-Cl)(cod)]$_2$ (0.150 g, 0.223 mmol) were reacted for 12 h in a dihloromethane/methanol mixture following the procedure described above. The resulting blue-green suspension was evaporated to dryness and the residue extracted with dichloromethane (3 × 15 mL), and the combined solutions were filtered through Celite. Work-up as above afforded the compound as green microcrystalline solid. Yield: 0.138 g (85%). Anal. Calcd for $C_{42}H_{54}Ir_4N_2O_2S_2$: C, 34.75; H, 3.75; N, 1.93; S, 4.42. Found: C, 34.80; H, 3.65; N, 2.01; S, 4.11. MS (FAB^{+}, CH_2Cl_2, *m*/*z*): 1452 (M^{+}, 69%), 1151 (M^{+} − Ir(cod), 62%). ^{1}H NMR ($CDCl_3$, 293 K) δ: 7.48 (dd, 2H, J_{H-H} = 7.2, J_{H-H} = 1.1 Hz), 6.85 (dd, 2H, J_{H-H} = 8.7 Hz, J_{H-H} = 7.2 Hz), 5.89 (dd, 2H, J_{H-H} = 8.70, J_{H-H} = 1.1 Hz) (pySO); 4.68 (m, 2H, =CH), 4.43 (m, 6H, =CH), 4.03 (m, 2H, =CH), 2.80 (m, 4H, =CH), 2.39 (m, 14H, >CH$_2$), 2.35 (m, 2H, =CH), 2.10 (m, 2H, >CH$_2$), 1.83 (m, 6H, >CH$_2$), 1.69 (m, 2H, >CH$_2$), 1.44 (m, 8H, >CH$_2$) (cod). $^{13}C\{^{1}H\}$ NMR ($CDCl_3$, 293 K) δ: 170.2 (C-O), 160.1 (C-S), 138.4, 118.1, 114.4 (CH) (pySO); 75.1, 71.3, 67.5, 66.1, 65.1, 64.5, 54.4, 49.1 (=CH, cod), 36.4, 32.2, 31.5, 31.2(2C), 30.9, 29.6, 29.1 (>CH$_2$, cod).

[Rh_4(μ-PySO)$_2$(CO)$_8$] (4). A solution of K_2PySO (0.386 mmol) in methanol (5 mL) was prepared following the procedure described above. The solvent was removed under vacuum, and the residue suspended in dichlomethane (10 mL). Solid [Rh(μ-Cl)(CO)$_2$]$_2$ (0.150 g, 0.386 mmol) was added under a carbon monoxide atmosphere to give a deep violet solution which was stirred for 1 h. The solution was filtered through Celite and then concentrated by continuous bubbling of carbon monoxide to about 1 mL. Slow addition of *n*-hexane (10 mL) and cooling to 258 K under carbon monoxide afforded the compound as violet microcrystals which were collected by filtration, washed with *n*-hexane, and then dried under vacuum. Yield: 0.139 g (81%). Anal. Calcd for $C_{18}H_6N_2O_{10}Rh_4S_2$: C, 24.40; H, 0.68; N, 3.16; S, 7.24. Found: C, 24.23; H, 0.78; N, 3.06; S, 7.46. MS (FAB^{+}, CH_2Cl_2, *m*/*z*): 885 (M^{+}, 22%), 829

($M^+ - 2CO$, 94%), 801 ($M^+ - 3CO$, 100%), 773 ($M^+ - 4CO$, 90%), 745 ($M^+ - 5CO$, 63%), 717 ($M^+ - 6CO$, 85%), 689 ($M^+ - 7CO$, 74%), 661 ($M^+ - 8CO$, 53%). ^{1}H NMR ($CDCl_3$, 293 K) δ: 6.82 (m, 4H), 5.98 (dd, 2H, J_{H-H} = 8.45, J_{H-H} = 0.97 Hz) (pySO). Calculated spectrum, δ: 6.791 (J_{H-H} = 6.99 Hz, J_{H-H} = 0.97 Hz), 6.842 (J_{H-H} = 6.99 Hz, J_{H-H} = 8.45 Hz), 5.980 (J_{H-H} = 8.45 Hz, J_{H-H} = 1.24 Hz). $^{13}C\{^1H\}$ NMR ($CDCl_3$, 293 K) δ: 184.9 (d, J_{Rh-C} = 62 Hz), 183.7 (d, J_{Rh-C} = 63 Hz), 182.5 (d, J_{Rh-C} = 72 Hz), 181.0 (d, J_{Rh-C} = 76 Hz) (CO); 170.2 (C-O), 152.7 (C-S), 139.6, 117.4, 115.1 (CH) (pySO). IR (CH_2Cl_2, cm^{-1}): 2099 (m), 2079 (s), 2068(s), 2029 (s), and 2013 (m).

[$Rh_4(\mu$-PySO)$_2$(cod)$_2$(CO)$_4$] (5). Carbon monoxide was bubbled through a solution of [$Rh_4(\mu$-PySO)$_2$(cod)$_4$] (**1**) (0.100 g, 0.091 mmol) in dichloromethane (15 mL) to give a deep violet solution of complex [$Rh_4(\mu$-PySO)$_2$(CO)$_8$] in 15 min. The solution was slowly concentrated under vacuum (5 mL) to give a deep red solution that was stirred under argon for 72 h. The dark blue solution obtained was concentrated under vacuum to about 1 mL to give a purple microcrystalline solid by slow addition of methanol (5 mL). The solid was collected by filtration, washed with methanol, and then dried under vacuum. Yield: 0.079 g (87%). Anal. Calcd for $C_{30}H_{30}N_2O_6Rh_4S_2$: C, 36.38; H, 3.05; N, 2.83; S, 6.47. Found: C, 36.02; H, 2.90; N, 2.84; S, 6.36. MS (FAB$^+$, CH_2Cl_2, m/z): 990 (M^+, 32%), 962 ($M^+ - CO$, 8%), 934 ($M^+ - 2CO$, 100%), 906 ($M^+ - 3CO$, 17%), 878 ($M^+ - 4CO$, 11%). ^{1}H NMR (C_6D_6, 293 K) δ: 6.86 (dd, 2H, J_{H-H} = 7.1; J_{H-H} = 0.9 Hz), 6.39 (dd, 2H, J_{H-H} = 8.45 Hz, J_{H-H} = 7.1 Hz), 6.00 (dd, 2H, J_{H-H} = 8.5 Hz, J_{H-H} = 0.9 Hz) (pySO); 4.98 (m, 2H, =CH), 4.85 (m, 2H, =CH), 4.28 (m, 2H, =CH), 3.27 (m, 2H, =CH), 2.60 (m, 4H, $>CH_2$), 2.14 (m, 4H, $>CH_2$), 2.02 (m, 2H, $>CH_2$), 1.77 (m, 2H, $>CH_2$), 1.46 (m, 4H, $>CH_2$) (cod). $^{13}C\{^1H\}$ NMR ($CDCl_3$, 293 K) δ: 187.6 (d, J_{Rh-C} = 64 Hz), 184.7 (d, J_{Rh-C} = 71 Hz) (CO); 171.0 (C-O), 157.4 (C-S), 138.9, 115.2, 113.9 (CH) (pySO); 90.4 (d, J_{Rh-C} = 12 Hz), 88.6 (d, J_{Rh-C} = 12 Hz), 73.2 (d, J_{Rh-C} = 12 Hz), 66.5 (d, J_{Rh-C} = 12 Hz) (=CH, cod); 35.0, 32.7, 27.9, 27.0 (CH_2, cod). IR (CH_2Cl_2, cm^{-1}): 2089 (sh), 2075 (s), 2057(m) y 2010 (s).

[$Rh_4(\mu$-PySO)$_2$(CO)$_4$(PPh$_3$)$_4$] (6). Method A. Carbon monoxide was bubbled through a solution of [$Rh_4(\mu$-PySO)$_2$(cod)$_4$] (0.150 g, 0.137 mmol) in dichloromethane (10 mL) for 15 min to give a deep violet solution of the complex [$Rh_4(\mu$-PySO)$_2$(CO)$_8$]. Further addition of PPh_3 (0.144 g, 0.548 mmol) gave a brown-reddish solution after evolution of carbon monoxide. The solution was stirred for 10 min and then concentrated under vacuum to about 1 mL. Slow addition of methanol (10 mL) gave the complex as a violet solid which was isolated by filtration, washed with methanol, and dried under vacuum. Yield: 0.169 g (68%).

Method B. A solution of K_2PySO (0.144 mmol) in methanol (5 mL) was added to a solution of *trans*-[RhCl(CO)(PPh$_3$)$_2$] (0.200 g, 0.290 mmol) in dichloromethane (15 mL) to give a red-brown solution which was stirred for 1 h. The solvent was removed under vacuum, and the residue dissolved in dichloromethane (15 mL) and then filtered through Celite. The solution was concentrated under vacuum to about 2 mL, and a violet solid began to crystallize. The crystallization was completed by addition of ethanol (10 mL), and the solid was collected by filtration, washed with methanol, and dried under vacuum. Yield: 0.087 g (66%). Anal. Calcd for $C_{86}H_{66}N_2O_6P_4Rh_4S_2$: C, 56.67; H, 3.65; N, 1.54; S, 3.52. Found C, 56.76; H, 3.57; N, 1.50; S, 3.48. MS (FAB$^+$, CH_2Cl_2, m/z): 1822 (M^+, 100%), 1794 ($M^+ - CO$, 5%), 1504 ($M^+ - PPh_3 - 2CO$, 5%), 1476 ($M^+ - PPh_3 - 3CO$, 5%), 1448 ($M^+ - PPh_3 - 4CO$, 5%), 1297 ($M^+ - 2PPh_3$, 56%), 1214 ($M^+ - 2PPh_3 - 3CO$, 16%), 1185 ($M^+ - 2PPh_3 - 4CO$, 24%). ^{1}H NMR ($CDCl_3$, 293 K) δ: 7.70−7.01 (m, 60 H) (PPh_3); 6.49 (d, 2H, J_{H-H} = 6.8 Hz), 6.15 (dd, 2H, J_{H-H} = 8.2 Hz, J_{H-H} = 6.8), 4.86 (d, 2H, J_{H-H} = 8.2) (pySO). $^{31}P\{^1H\}$ NMR ($CDCl_3$, 293 K) δ: 39.76 (d, J_{Rh-P} = 163 Hz), 38.69 (d, J_{Rh-P} = 175 Hz). IR (CH_2Cl_2, cm^{-1}): 1982 (s), 1974 (sh).

[$Rh_4(\mu$-PySO)$_2$(cod)$_4$][CF_3SO_3] ($\mathbf{1a}^+$**).** Solid $AgCF_3SO_3$ (0.071 g, 0.274 mmol) was added to a solution of [$Rh_4(\mu$-PySO)$_2$(cod)$_4$] (**1**) (0.300 g, 0.274 mmol) in dichloromethane (15 mL), and the mixture was stirred for 1 h with exclusion of light. The dark suspension was filtered through Celite under argon to remove the metallic silver, and the resulting bright garnet solution concentrated under vacuum to about 1 mL. Slow addition of diethyl ether (10 mL) gave $\mathbf{1a}^+$ as a garnet microcrystalline solid. Yield: 0.268 g (79%). Anal. Calcd for $C_{43}H_{54}F_3N_2O_5Rh_4S_3$: C, 41.53; H, 4.38; N, 2.25; S, 7.73. Found: C, 41.25; H, 4.09; N, 2.17; S, 7.65. MS (FAB$^+$, CH_2Cl_2, m/z): 1094 (M^+, 72%), 986 ($M^+ -$ cod, 8%), 883 ($M^+ -$ Rh(cod), 37%), 758 ($M^+ -$ Rh(cod) − pySO, 15%). Λ_M (Ω^{-1} cm^2 mol^{-1}): 109 (acetone, 4.85×10^{-4} M).

[$Rh_4(\mu$-PySO)$_2$(cod)$_4$][PF_6] ($\mathbf{1b}^+$**).** Solid [Cp_2Fe]PF_6 (0.045 g, 0.137 mmol) was added to a solution of [$Rh_4(\mu$-PySO)$_2$(cod)$_4$] (**1**) (0.150 g, 0.137 mmol) in dichloromethane (15 mL). The mixture was stirred for 30 min, and the resulting bright garnet solution concentrated under vacuum to about 3 mL. Slow addition of diethyl ether (10 mL) gave $\mathbf{1b}^+$ as a garnet microcrystalline solid that was collected by filtration, washed repeatedly with diethyl ether, and then vacuum-dried. Yield: 0.132 g (78%). Anal. Calcd for $C_{42}H_{54}F_6N_2O_2PRh_4S_2$: C, 40.70; H, 4.39; N, 2.26; S, 5.17. Found: C, 40.58; H, 4.28; N, 2.24; S, 5.15. MS (FAB$^+$, CH_2Cl_2, m/z): 1094 (M^+, 72%), 883 ($M^+ -$ Rh − cod, 37%), 758 ($M^+ -$ Rh(cod) − pySO, 15%). Λ_M (Ω^{-1} cm^2 mol^{-1}): 118 (acetone, 5.6×10^{-4} M).

[$Rh_4(\mu$-PySO)$_2$(tfbb)$_4$][CF_3SO_3] ($\mathbf{2}^+$**).** [$Rh_4(\mu$-PySO)$_2$(tfbb)$_4$] (0.100 g, 0.064 mmol) and $AgCF_3SO_3$ (0.017 g, 0.064 mmol) were reacted in dichloromethane (15 mL) for 1 h with exclusion of light to give a purple solution. Work-up as described above gave the compound as a purple microcrystalline solid. Yield: 0.095 g (87%). Anal. Calcd for $C_{59}H_{30}F_{19}N_2O_5Rh_4S_3$: C, 41.30; H, 1.76; N, 1.63; S, 5.61. Found: C, 41.15; H, 1.53; N, 1.59; S, 5.56. MS (FAB$^+$, CH_2Cl_2, m/z): 1566 (M^+, 100%), 1340 ($M^+ -$ tfbb, 20%). Λ_M (Ω^{-1} cm^2 mol^{-1}): 102 (acetone, 4.92×10^{-4} M).

[$Ir_4(\mu$-PySO)$_2$(cod)$_4$][CF_3SO_3] ($\mathbf{3}^+$**).** [$Ir_4(\mu$-PySO)$_2$(cod)$_4$] (0.100 g, 0.069 mmol) and $AgCF_3SO_3$ (0.018 g, 0.069 mmol) were reacted in dichloromethane (15 mL) for 1 h with exclusion of light to give a green suspension. Work-up as describe above gave the compound as a green microcrystalline solid. Yield: 0.074 g (67%). Anal. Calcd for $C_{43}H_{54}F_3Ir_4N_2O_5S_3$(%): C, 32.26; H, 3.40; N, 1.75; S, 6.01. Found: C, 32.01; H, 3.32; N, 1.73; S, 6.08. MS (FAB$^+$, CH_2Cl_2, m/z): 1452 (M^+, 100%), 1152 ($M^+ -$ Ir(cod), 29%), 743 ($M^+ - 2$Ir − 3cod, 21%). Λ_M (Ω^{-1} cm^2 mol^{-1}): 105 (acetone, 2.99×10^{-4} M).

Crystal Structure determination of [$Rh_4(\mu$-PySO)$_2$(cod)$_4$] (1). Single crystals for the X-ray diffraction study of compound **1** were obtained by slow diffusion of ethanol into a dichloromethane solution of the complex at 258 K. Crystal data for **1**: $C_{42}H_{54}N_2O_2Rh_4S_2 \cdot 2(CH_2Cl_2)$, fw 1264.48, space group $C2/c$, a = 9.3868(11), b = 18.516(2), c = 25.869(3) Å, β = 98.994(2)°, V = 4441.0(9) Å^3, Z = 4, D_{calcd} 1.891 g cm^{-3}, μ = 1.836 mm^{-1}. X-ray data were collected for an irregular block (0.24 × 0.20 × 0.11 mm) at low temperature (100(2) K) on a Bruker SMART APEX CCD difractometer. Data were collected using graphite-monochromated Mo Kα radiation (λ = 0.71073 Å; 7268 measd. reflns. ($2.2 \le \theta \le 28.47°$), 5191 unique ($R_{int}$ = 0.0351)). An absorption correction for **1** was applied by using the SADABS routine[38] (min, max. transm. factors 0.6598, 0.8194). The structure was solved by direct methods, completed by subsequent difference Fourier techniques and refined by full-matrix least-squares on F^2 (SHELXL-97)[39] with initial isotropic thermal parameters. Anisotropic thermal parameters were used in the last cycles of refinement for all non-hydrogen atoms (no. data/restraints/parameters 5191/0/291). Two solvent molecules of dichloromethane were found. All hydrogens were found in the difference

(38) (a) *SADABS: Area detector absorption*; Bruker-AXS: Madison, WI, 1996.(b) Blessing, R. H. *Acta Crystallogr., Sect. A* **1995**, *51*, 33.

(39) Sheldrick, G. M. *SHELXL-97 Program for Crystal Structure Refinement*; University of Göttingen: Göttingen, Germany, 1997.

Fourier maps and refined with positional parameters riding on carbon atoms, but with free displacement parameters. Final agreement factors were $R_1(F)$ ($F^2 \geq 2\sigma(F^2)$) 0.0412, $wR_2(F^2)$ 0.0955 and GOF 1.044.

Acknowledgment. The financial support from Ministerio de Educación y Ciencia (MEC/FEDER) Project CTQ2006-03973/BQU and Grant CSD2006-0015 Consolider Ingenio 2010 is gratefully acknowledged.

Supporting Information Available: An X-ray crystallographic file in CIF format for the structure determination of complex $[Rh_4(\mu\text{-}PySO)_2(cod)_4]$ (**1**). This material is available free of charge via the Internet at http://pubs.acs.org.